Natural Resources for Human Health
eISSN: 2583-1194

Original Research

Received 16 July 2026
Revised 17 Aug 2026
Accepted 03 Sep 2026

Natural Resources for Human Health 2026, Vol. 6 (20s): 1470–1483

KEYWORDS:
ATR-FTIR; human scalp hair; molecular profiling; forensic hair analysis; keratin

Molecular Characterization of Human Scalp Hair Using ATR-FTIR Spectroscopy: Implications for Hair Health and Biological Assessment

Shreya[1], Sankeerthana Renukaprasad[2], Pramod Mallikarjunaswamy[3], Lakshmi Vijay Kurbet[1], Thaniya Poovamma[4], Komal Kumar Javarappa[2,*]

[1]Department of Pharmaceutical Chemistry, JSS Academy of Higher Education and Research (JSS AHER), Mysuru, Karnataka, India.
[2]University Sophisticated Instrumentation Center (USIC), JSS Academy of Higher Education and Research (JSS AHER), Mysuru, Karnataka, India.
[3]Division of Biochemistry, School of Life Sciences, JSS Academy of Higher Education and Research (JSS AHER), Mysuru, Karnataka, India.
[4]Department of Nutrition and Dietetics, , JSS Academy of Higher Education and Research (JSS AHER), Mysuru, Karnataka, India.
[*]Corresponding author: Komal Kumar Javarappa
University Sophisticated Instrumentation Center (USIC), JSS Academy of Higher Education and Research (JSS AHER), Mysuru, Karnataka, India. Email: komalkumar@jssuni.edu.in

ABSTRACT: Human scalp hair contains keratin proteins, lipids, and other biochemical constituents that may provide useful molecular information for forensic analysis. This study aimed to characterize the spectral profile of human scalp hair using attenuated total reflectance Fourier transform infrared (ATR-FTIR) spectroscopy and evaluate spectral similarities and variations among individuals with different demographic characteristics and scalp conditions. Nine hair specimens collected from five males and four females across different age groups and scalp conditions were analysed using a PerkinElmer Spectrum Two FT-IR spectrometer equipped with a diamond ATR crystal. Spectral data were acquired over 4000–400 cm^{-1} at a resolution of 4 cm^{-1} using 32 co-added scans, followed by baseline correction, normalization, and ATR correction. The spectra consistently demonstrated characteristic absorption bands corresponding to Amide I (1630–1634 cm^{-1}), Amide II (1513–1537 cm^{-1}), Amide III (1232–1236 cm^{-1}), and lipid-associated CH_2 stretching vibrations (2920–2923 and 2851–2856 cm^{-1}). Comparatively greater spectral variation was observed within the 1200–900 cm^{-1} fingerprint region, whereas the major spectral features were broadly similar between male and female specimens. The specimen from an individual with androgenetic alopecia retained the principal absorption features observed across the dataset. These preliminary findings suggest that ATR-FTIR spectroscopy may offer a rapid and minimally destructive approach for molecular characterization of human scalp hair. Further studies involving larger cohorts, replicate measurements, and quantitative chemometric analyses are necessary to establish its reproducibility and forensic applicability.

1. INTRODUCTION

Human hair is a unique and durable biological matrix that retains molecular and biochemical information over extended periods, making it relevant to retrospective biological and chemical investigations . It is a keratinized tissue produced by the hair follicle and is composed predominantly of α-keratin proteins arranged in a highly organized hierarchical structure, together with water,

melanin pigments, structural lipids, and surface-associated lipids (Bragulla & Homberger, 2009; Yang et al., 2014) . The cortex, which constitutes the major portion of the hair fiber, contains closely packed keratin intermediate filaments stabilized by disulfide cross-links, whereas the cuticle consists of overlapping layers that contribute to the mechanical integrity and protection of the fiber (Fernandes et al., 2023; Malinauskyte et al., 2021) . This complex molecular organization allows hair to preserve biochemical features associated with both endogenous biological processes and exposure to external influences (Florou et al., 2025; Philipsen et al., 2021) .

The biochemical and structural characteristics of hair can vary according to intrinsic factors such as sex, age, genetic background, ethnicity, and endocrine status, as well as extrinsic factors including cosmetic treatments, ultraviolet radiation, environmental exposure, nutritional status, and lifestyle practices (Boo, 2024; Hussein et al., 2025) . Sex-related variation in hair characteristics has therefore received attention in forensic, cosmetic, endocrinological, and biomedical research (Cedirian et al., 2025) . Previous studies have reported differences between male and female hair fibers in parameters such as fiber diameter, tensile properties, growth characteristics, lipid distribution, and surface morphology(Abed et al., 2024; Kaleta et al., 2021) . These differences may reflect variation in hair morphology, biochemical composition, follicular biology, and environmental or cosmetic exposure. Hormonal factors, including androgenic and estrogenic signalling, may contribute to some aspects of hair-follicle and hair-fiber biology; however, the relative contribution of hormonal and non-hormonal factors remains context-dependent (Grymowicz et al., 2020; Szöllősi et al., 2017) .

Attenuated Total Reflectance Fourier Transform Infrared (ATR-FTIR) spectroscopy is a useful analytical approach for the molecular characterization of biological materials because it requires minimal sample preparation and enables rapid, non-destructive spectral acquisition (Cruz et al., 2016; Hu et al., 2012) . The technique provides vibrational information associated with functional groups present in proteins, lipids, carbohydrates, and other molecular constituents (Zhou et al., 2024) . In hair analysis, the limited penetration of the ATR evanescent wave enables interrogation of the near-surface region of the hair fiber, including the cuticle and outer cortical regions, which may be influenced by biochemical composition and external exposure (Kalmodia et al., 2015; Mitu, Cerda, et al., 2023) . ATR-FTIR therefore provides an opportunity to examine the characteristic molecular features of hair and to assess similarities and differences among individual samples (Portaccio et al., 2023) .

When combined with appropriate spectral preprocessing and analytical approaches, ATR-FTIR spectroscopy can generate molecular spectral profiles that reflect the major biochemical constituents of human hair (Zhao et al., 2023) . Such profiles may be relevant to forensic investigations in which hair is encountered as trace biological evidence and to biomedical studies investigating variation in hair composition(Chatterley et al., 2022; Mehra & Chadha, 2020) . Although spectroscopic approaches have increasingly been applied to hair research, studies specifically examining the ATR-FTIR spectral characteristics of human scalp hair across different individual and scalp conditions remain limited (Ji et al., 2020; Swamy et al., 2025) . Establishing well-characterized reference spectra is therefore important for understanding the molecular features and sources of spectral variation observed in human hair (Gvazava et al., 2023; Malek et al., 2014) .

The present work employed ATR-FTIR spectroscopy to characterize the molecular fingerprint of human scalp hair obtained from individuals with varying scalp conditions (Dragojlov et al., 2025; Pienpinijtham et al., 2018) . Particular emphasis was placed on identifying characteristic absorption bands and spectral features associated with major biochemical constituents of hair, including keratin proteins, lipids, and sulfur-containing compounds (Sharma et al., 2020; Zha et al., 2019) . Qualitative comparisons were also undertaken to examine the observed spectral features among samples representing different scalp conditions, including dandruff, mild hair fall, and clinically confirmed androgenetic alopecia (Holman & Kurouski, 2023a; Madel et al., 2016) . Through ATR-FTIR-based molecular profiling, the study provides preliminary observations of the spectral characteristics of human scalp hair and establishes a basis for further investigation using larger sample sets and quantitative analytical approaches (Mitu, Trojan & Halámková 2023; Javarappa, … & 2026) .

2. MATERIALS AND METHODS

2.1 Hair Sample Collection and Preparation

A total of nine human scalp hair samples (five males and four females) representing different age groups and scalp conditions, including healthy individuals, dandruff, mild hair fall, and clinically confirmed androgenetic alopecia, were included in this research work. Hair samples measuring 3-12 cm in length were collected from the posterior vertex and occipital regions of the scalp. Fresh hair strands were plucked using sterile gloves to minimize contamination and immediately subjected to analysis.

The samples were cut into small, uniform segments to ensure optimal contact with the ATR crystal surface. Intrinsic factors such as age, sex, and scalp condition were noted, detailed information regarding extrinsic factors, including cosmetic treatments, medication use, and environmental exposures, was not systematically documented.

2.2 ATR-FTIR Spectroscopic Analysis

ATR-FTIR analysis was performed using a PerkinElmer Spectrum Two FT-IR spectrometer equipped with a diamond ATR crystal. Spectra were acquired over the 4000-400 cm^{-1} range at a 4 cm^{-1} resolution using 32 co-added scans per sample. A constant pressure of about 70 psi was applied to ensure adequate sample-crystal contact, and background spectra were recorded before each analysis. Spectral preprocessing, including baseline correction, normalization, and ATR correction, was carried out using Spectrum 10 software. Functional group assignments were made based on characteristic absorption bands and comparison with published literature.

2.3 Statistical Analysis

Due to the exploratory nature of the study and the limited sample size (n = 9; 4-female and 5-male), data interpretation was primarily descriptive. Associations between spectral features, scalp conditions, and follicular integrity were qualitatively assessed through comparative evaluation of ATR-FTIR profiles.

3. RESULTS AND DISCUSSION

3.1 Spectral data interpritation

The demographic, morphological, and sampling characteristics of the nine human scalp hair specimens are illustrated in Table 1. The study included specimens from different age groups and scalp conditions, comprising healthy hair, dandruff, mild hair fall, and one clinically confirmed androgenetic alopecia (AGA) specimen. Hair thickness ranged from 68 to 88µm, and specimens were collected from either the posterior vertex or occipital region. The ATR-FTIR spectra obtained from all nine specimens are presented as an overlay in Figure 1, demonstrating the overall spectral characteristics and inter-individual variation observed within the study population. Across the analysed specimens, the spectra exhibited broadly comparable major absorption features. A broad absorption band within the 3600–3200 cm^{-1} region was consistently observed and was assigned to overlapping O–H and N–H stretching vibrations. Distinct absorption bands were detected at 2920–2923 and 2851–2856 cm^{-1}, corresponding to asymmetric and symmetric CH_2 stretching vibrations, respectively. The principal protein-associated absorption bands were observed at 1630–1634 cm^{-1} and 1513–1537 cm^{-1}, corresponding to Amide I and Amide II vibrations, respectively. Additional bands occurring at 1450–1456 cm^{-1} were associated with CH_2/CH_3 deformation vibrations, whereas the absorption features at 1232–1236 cm^{-1} corresponded to Amide III or peptide-associated vibrations. The major spectral regions and their corresponding molecular assignments are summarized in Table 2, while the characteristic absorption frequencies identified for individual specimens are presented in Table 3. Greater spectral variation was observed within the fingerprint region extending from approximately 1200 to 900 cm^{-1}. Several specimens exhibited absorption bands between 1042 and 1081 cm^{-1}, which were associated with C–O-containing and other overlapping molecular vibrations. Additional weak absorption features were observed between 950 and 970 cm^{-1} in selected specimens. Owing to the potential overlap of multiple molecular contributions within this region, these spectral features were interpreted with caution and were not assigned to a single specific molecular component. The spectra of the female specimens (F1–F4) are presented in Figure 2, while those of the male specimens (M1–M5) are presented in Figure 3. Both groups displayed the principal absorption regions identified in the overall spectral dataset, including the characteristic Amide I, Amide II, Amide III, and CH_2-associated bands. The major spectral profile was therefore broadly conserved across the female and male specimens. The single AGA specimen (M4) similarly exhibited the principal absorption features observed among the other analysed specimens. No additional major absorption band unique to the M4 specimen was identified within the analysed spectral range.

Table 1. Morphological and regional characteristics of analysed hair samples across diverse age groups and scalp conditions

Sample code	Age group (years)	Condition	Hair Thickness (µm)	Collected region of the hair samples
F1	20-25	Healthy	82	Posterior Vertex

F2	20-25	Healthy	84	Occipital Region
F3	26-30	Dandruff	88	Posterior Vertex
F4	31-35	Healthy	68	Posterior Vertex
M1	18-25	Mild hair fall	75	Posterior Vertex
M2	26-30	Healthy	78	Posterior Vertex
M3	20-25	Healthy	70	Posterior Vertex
M4	36-40	Androgenic Alopecia	69	Posterior Vertex
M5	20-25	Healthy	85	Occipital Region

Table 2. ATR-FTIR spectral regions and their corresponding functional groups in human scalp hair.

Spectral region (cm^{-1})	**Major vibrational assignment**	**Tentative biochemical constituent in human hair**	**Reference**
3600–3200	Broad O–H and N–H stretching vibrations	Bound water and hydrogen-bonded N–H groups associated with keratin	(Brzózka & Kolodziejski 2017; Li et al. no date; Mujeeb, Technol & 2017)
2980–2950	C–H stretching, predominantly CH_3 asymmetric stretching	Lipid alkyl chains and aliphatic side chains	(Li et al., n.d.; Mujeeb et al., n.d.; Pienpinijtham et al., 2018)
2930–2900	CH_2 asymmetric stretching	Long-chain aliphatic lipids and fatty-acid residues	(Holman & Kurouski, 2023b; Li et al.; Mujeeb et al., n.d.; Pienpinijtham et al., 2018)
2860–2840	CH_2 symmetric stretching	Structural and surface-associated lipids	(Pienpinijtham et al. 2018; Holman & Kurouski 2023b; Li et al.; Mujeeb et al.)
1650–1620	Amide I; predominantly peptide C=O stretching	Keratin protein backbone and α-keratin secondary structure	(Pienpinijtham et al. 2018; Holman & Kurouski 2023b; Li et al.; Mujeeb et al.)
1550–1510	Amide II; N–H bending coupled with C–N stretching	Keratin and other peptide/protein components	(Pienpinijtham et al. 2018; Holman & Kurouski 2023b; Li et al.; Mujeeb et al.)
`1260–1200	Amide III; coupled C–N stretching and N–H bending	Keratin-associated peptide structure	(Pienpinijtham et al. 2018; Holman & Kurouski 2023b; Li et al.; Mujeeb et al.)
1100–1000	C–O stretching and other fingerprint-region vibrations	Carbohydrate-associated components and other oxygen-containing molecular groups	(Brzózka & Kolodziejski 2017; Li et al. no date; Mujeeb, Technol & 2017)

1080–1030	C–O and, where supported by the spectrum, S–O-related vibrations	Oxygen-containing groups and potentially oxidised sulphur-containing species	(Li et al., n.d.; Mujeeb et al., n.d.; Pienpinijtham et al., 2018)
970–950	Weak bands potentially associated with phosphate-containing or other molecular vibrations	Tentative phosphate-associated or other minor molecular components	(Pienpinijtham et al. 2018; Holman & Kurouski 2023b; Li et al.; Mujeeb et al.)

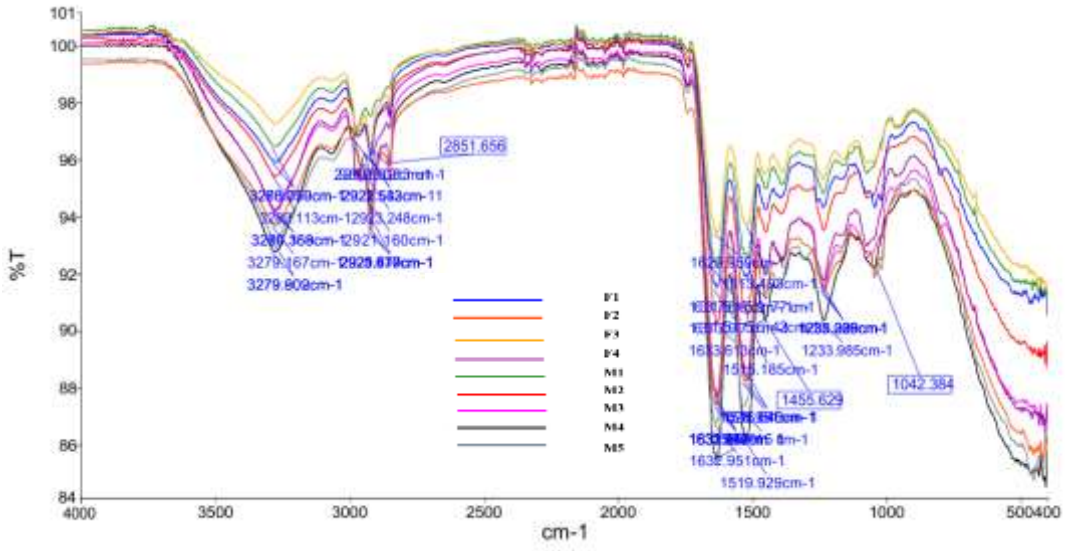
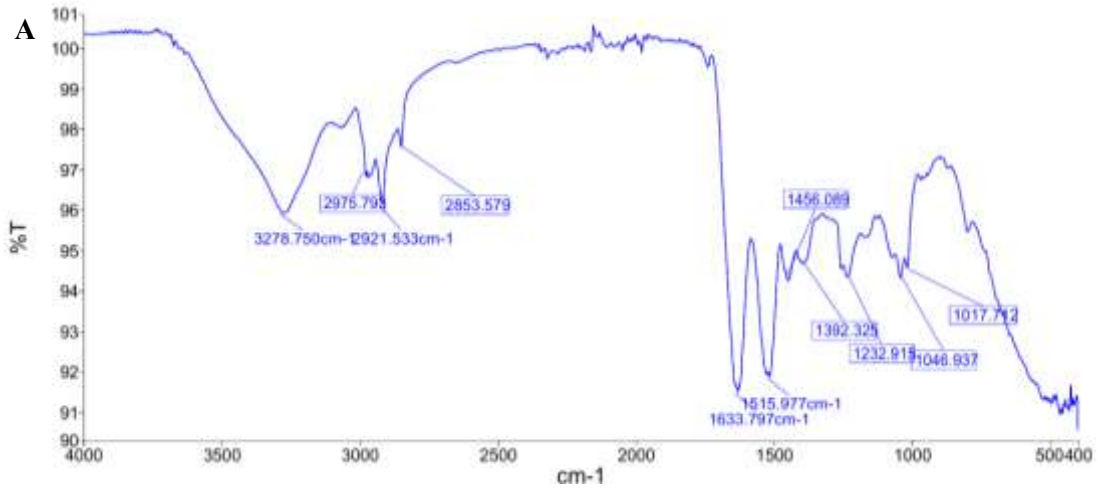
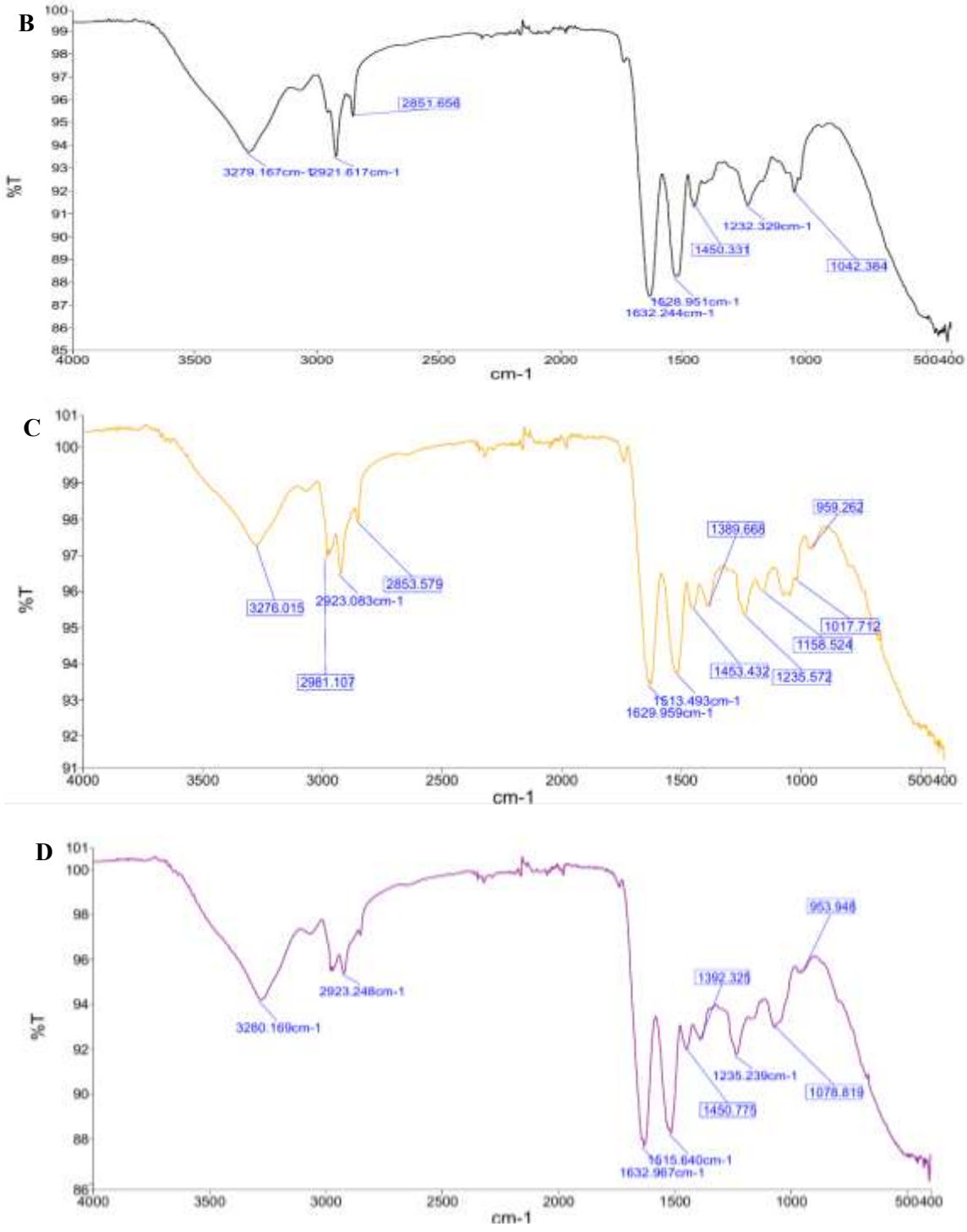
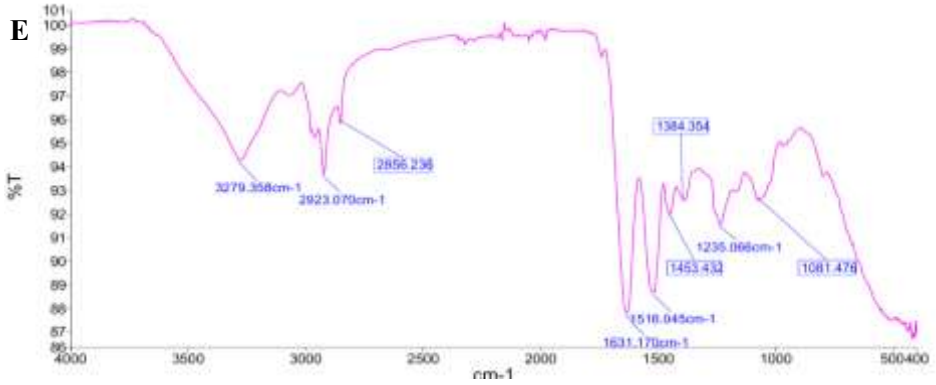


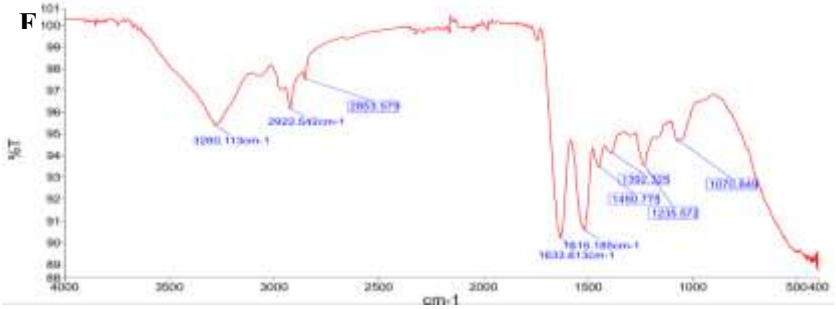
Figure 1. ATR-FTIR spectra of human scalp hair specimens. Overlay of ATR-FTIR spectra obtained from all nine analyzed human scalp hair samples (F1–F4 and M1–M5), showing the overall similarity of the major absorption bands associated with protein-, lipid-, and other molecular components of the hair matrix.

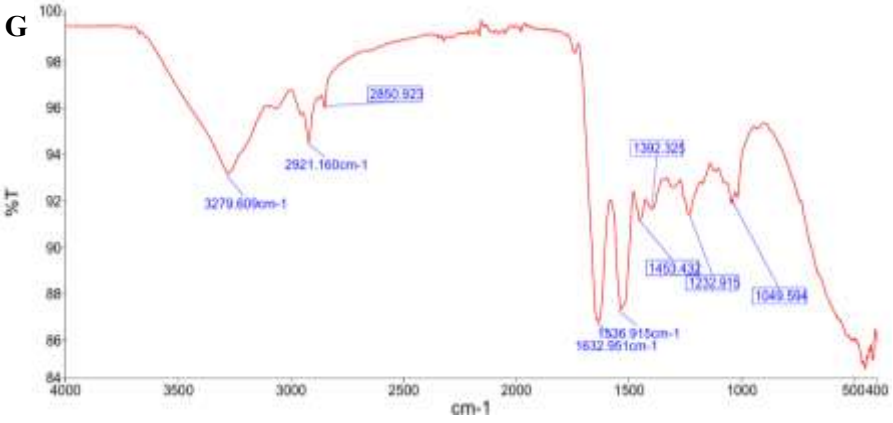


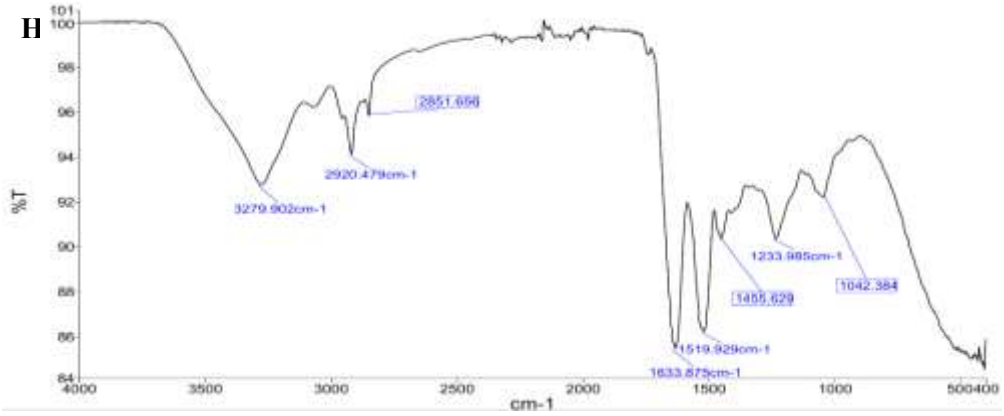
Natural Resources for Human Health
eISSN: 2583-1194




E
%T
3279.358cm-1
2923.070cm-1
2856.236
1384.354
1453.432
1235.066cm-1
1081.476
1516.045cm-1
1631.170cm-1
cm-1


F
%T
2922.542cm-1
2853.579
1392.325
1460.778
1235.673
1070.849
1633.413cm-1
cm-1


G
%T
3279.609cm-1
2921.160cm-1
2850.923
1392.325
1460.432
1232.919
1049.594
1536.915cm-1
1632.961cm-1
cm-1


H
%T
3279.902cm-1
2920.479cm-1
2851.656
1233.985cm-1
1455.629
1042.384
1519.929cm-1
1633.875cm-1
cm-1

Natural Resources for Human Health
eISSN: 2583-1194

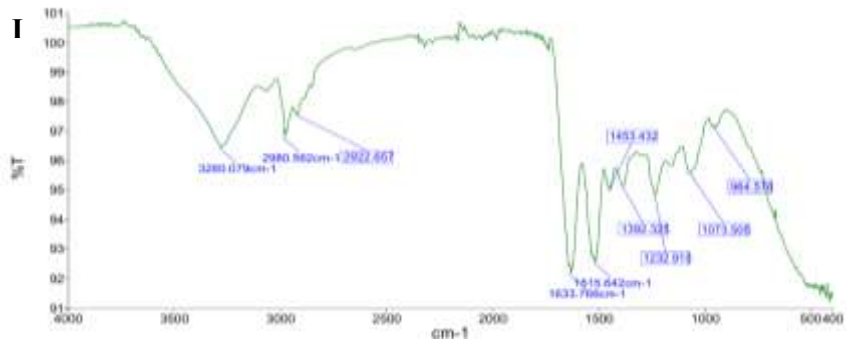


Figure 1. ATR-FTIR spectra of human scalp hair specimens. Overlay of ATR-FTIR spectra obtained from all nine analysed human scalp hair samples (F1–F4: A-D and M1–M5:E-I), showing the overall similarity of the major absorption bands associated with protein-, lipid-, and other molecular components of the hair matrix.

Table 3. Characteristic ATR-FTIR absorption frequencies of female and male human scalp hair specimens. Observed peak positions (cm^{-1}) and their corresponding vibrational assignments are presented for samples F1–F4 and M1–M5.

Hair	Spectral region (cm^{-1})	Functional Group	Reference
F1	3279,2976,2922,2854,1634, 1516,1456,1392,1233,1047,1018.	O–H/N–H stretching, C–H_3/C–H_2 aliphatic C–H stretching, Amide I (C=O), Amide II (N–H), CH_2/CH_3 bending, Amide III, C–O Stretching, S–O/C–O vibrations	(Brzózka & Kolodziejski 2017; Li et al. no date; Mujeeb, Technol & 2017)
F2	3279,2922,2852,1632,1529, 1450,1232,1042.	Broad O–H/N–H stretching, aliphatic C–H_2/C–H stretching, Amide I(C=O), Amide II(N–H), CH_2/CH_3 bending, Amide III, C–O stretching	(Li et al., n.d.; Mujeeb et al., n.d.; Pienpinijtham et al., 2018)

F3	3276,2981,2923,2854,1630, 1513,1453,1390,1236,1159, 1018,959.	Broad O–H/N–H stretching, C–H_3/CH_2 aliphatic C–H stretching, Amide I(C=O), Amide II(N–H), CH_2/CH_3 bending, CH_3 bending, Amide III, C–O–C stretching, S–O/C–O vibrations, PO_4^{3-} vibrations	(Holman & Kurouski, 2023b; Li et al.; Mujeeb et al., n.d.; Pienpinijtham et al., 2018)
F4	3280, 2923, 1633, 1516, 1451, 1392, 1235, 1079, 954.	Broad O–H/N–H, C–H aliphatic stretching, Amide I(C=O), Amide II(N–H), CH_2/CH_3 bending, CH_3 bending, Amide III, S–O/C–O vibrations,PO_4^{3-} vibrations	(Pienpinijtham et al. 2018; Holman & Kurouski 2023b; Li et al.; Mujeeb et al.)
M1	3279, 2923, 2856, 1631, 1516, 1453, 1384, 1235, 1081, 964.	Broad O–H/N–H stretching, aliphatic C–H stretching, Amide I(C=O), Amide II(N–H), CH_2/CH_3 bending, Amide III, C–O stretching, C–S/C–C vibration	(Pienpinijtham et al. 2018; Holman & Kurouski 2023b; Li et al.; Mujeeb et al.)
M2	3280, 2923, 2854, 1634, 1515, 1451, 1392, 1236, 1071	Broad O–H/N–H stretching, aliphatic C–H stretching, Amide I(C=O), Amide II(N–H), CH_2/CH_3 bending, Amide III, S–O / C–O stretching	(Pienpinijtham et al. 2018; Holman & Kurouski 2023b; Li et al.; Mujeeb et al.)
M3	3280, 2921, 2851,1633, 1537, 1453, 1392, 1233, 1050.	Broad O–H/N–H stretching, aliphatic C–H stretching, Amide I(C=O), Amide II(N–H),	(Pienpinijtham et al. 2018; Holman & Kurouski 2023b; Li et al.; Mujeeb et al.)

		CH_2/CH_3 bending, Amide III, C–O stretching	
M4	3280,2920, 2852, 1634, 1520, 1456, 1234, 1042	Broad O–H/N–H stretching, aliphatic C–H stretching, Amide I(C=O), Amide II(N–H), CH_2 bending, Amide III, C–O stretching	(Brzózka & Kolodziejski 2017; Li et al. no date; Mujeeb, Technol & 2017)
M5	3280, 2981, 2923, 1634, 1516, 1453, 1392, 1233, 1074, 965.	O–H/N–H stretching, C–H_3/C–H_2 aliphatic C–H stretching, Amide I(C=O), Amide II(N–H), CH_2/CH_3 bending, Amide III, C–O stretching, PO_4^{3-} vibrations	(Li et al., n.d.; Mujeeb et al., n.d.; Pienpinijtham et al., 2018)

3.2 Discussion

The ATR-FTIR spectra demonstrated a broadly conserved molecular profile among the nine human scalp hair specimens analysed. The major bands were associated with protein, lipid, and other molecular components of the hair matrix, consistent with previous FTIR studies of human hair and keratin-based materials (Mujeeb, Technol & 2017 no date) . The bands at approximately 1630-1634 cm^{-1} and 1513-1537 cm^{-1} corresponded to Amide I and Amide II vibrations, respectively, reflecting the protein-rich nature of the hair samples (Brzózka & Kolodziejski, 2017; Li et al., n.d.) . The CH_2 stretching bands around 2920-2923 and 2851-2856 cm^{-1} were consistent with aliphatic lipid-associated components (Al-Kelani & Buthelezi, 2024; Holman & Kurouski, 2023b) . The Amide III/peptide-associated region around 1232-1236 cm^{-1} further supported the presence of keratin-associated molecular features. Larger differences occurred within the 1200-900 cm^{-1} of the fingerprint region, where overlapping contributions from several functional groups could possibly occur. Although some bands in this region may be associated with sulphur-containing or oxidised sulphur species, ATR-FTIR alone does not allow definitive identification of specific sulphur-containing compounds. Consequently, these assignments were regarded as provisional (Kathiresan & Meenakshisundaram, 2022) .

Comparison of the spectra in Figures 2 and 3 showed that the major spectral features were broadly similar between the female and male specimens. However, due to the limited sample counts, these observations do not establish sex-specific spectral differences. Similarly, the single AGA specimen (M4) displayed the major spectral features observed across the dataset. Since only one AGA specimen was analysed, this observation cannot be considered representative of AGA or used to identify a condition-specific spectral signature. From a forensic perspective, the present findings demonstrate the feasibility of obtaining a rapid and minimally destructive molecular profile of human scalp hair using ATR-FTIR spectroscopy. The present findings demonstrate the potential of ATR-FTIR spectroscopy for rapid, minimally destructive characterization of the molecular features of human scalp hair and provide a preliminary spectral reference for future forensic investigations. The consistent identification and characterization of protein- and lipid-associated bands across the analysed male and female specimens supports the significance of ATR-FTIR as an initial screening and profiling approach for hair samples. Although the present dataset is limited by the limited sample size, unequal representation of scalp conditions, and inclusion of only one clinically confirmed androgenetic alopecia (AGA) specimen, these findings provide a foundation for subsequent studies involving larger and more

diverse cohorts. Future investigations incorporating replicate measurements, standardized documentation of external hair treatments and exposures, multiple AGA cases, and quantitative chemometric analysis may further determine the reproducibility and forensic applicability of the observed spectral variations. Accordingly, the present study should be regarded as an initial characterization study that establishes a basis for more extensive validation of ATR-FTIR-based molecular profiling of human scalp hair.

4. CONCLUSION

he present study demonstrates the feasibility of ATR-FTIR spectroscopy as a rapid and minimally destructive approach for characterizing the molecular features of human scalp hair. Across the nine analyzed specimens, consistent spectral features corresponding to keratin-associated Amide I, Amide II, and Amide III vibrations were observed, together with lipid-associated C–H stretching bands and variable features within the fingerprint region. The overall similarity of the major spectral profiles indicates that ATR-FTIR can provide a characteristic molecular representation of human scalp hair, while the observed variations highlight the complexity of the hair matrix and the influence of individual and scalp-related factors. The findings provide preliminary spectral observations that may serve as a reference for future forensic and biomedical investigations involving hair analysis. However, interpretation is limited by the small sample size, unequal representation of scalp conditions, and inclusion of only one clinically confirmed androgenetic alopecia specimen. Therefore, the present findings should be considered exploratory rather than population-level evidence. Further studies involving larger and well-characterized cohorts, multiple AGA specimens, replicate measurements, standardized documentation of external exposures, and quantitative chemometric analysis are warranted to establish the reproducibility and forensic applicability of ATR-FTIR-based molecular profiling of human scalp hair.

ACKNOWLEDGEMENTS

The authors acknowledge the technical assistance provided by the University Sophisticated Instrumentation Centre(USIC), JSS AHER, Mysuru.

AUTHOR CONTRIBUTIONS

Sreya: Formal analysis; Writing-original draft; Writing-review & editing

Sankeerthana Renukaprasad: Data curation; Formal analysis; Interpretation; Writing-original draft

Pramod Mallikarjunaswamy: Formal analysis; Interpretation; Formatting

Lakshmi Vijay Kurbet: Writing-original draft

Thaniya Poovamma: Formal analysis

Komal Kumar Javarappa: Supervision; Formal analysis; Visualization; Writing-review & editing.

†**Equal Contribution Statement:** Authors Shreya and Sankeerthana Renukaprasad have equally contributed to the work and share equal first authorship.

CONFLICT OF INTEREST

The authors declare that there is no conflict of interest.

ETHICS STATEMENT

Ethical approval was not required for this study.

DATA AVAILABILITY STATEMENT

Data supporting the findings of this study are available from the corresponding author upon reasonable request.

REFERENCES

[1] Abed, M.S., Moosa, A.A., Alzuhairi, M.A., 2024. Heavy metals in cosmetics and tattoos: a review of historical background, health impact, and regulatory limits. Journal of Hazardous Materials Advances 13, 100390. https://doi.org/10.1016/j.hazadv.2023.100390.

[2] Al-Kelani, M., Buthelezi, N., 2024. Advancements in medical research: Exploring Fourier Transform Infrared (FTIR) spectroscopy for tissue, cell, and hair sample analysis. Skin Research and Technology 30(6), e13733. https://doi.org/10.1111/srt.13733.
[3] Boo, Y.C., 2024. Intrinsic and Extrinsic Factors Associated with Hair Graying (Canities) and Therapeutic Potential of Plant Extracts and Phytochemicals. Applied Sciences 14(17), 7450. https://doi.org/10.3390/app14177450.
[4] Bragulla, H.H., Homberger, D.G., 2009. Structure and functions of keratin proteins in simple, stratified, keratinized and cornified epithelia. Journal of Anatomy 214(4), 516–559. https://doi.org/10.1111/j.1469-7580.2009.01066.x.
[5] Brzózka, P., Kolodziejski, W., 2017. Sex-related chemical differences in keratin from fingernail plates: a solid-state carbon-13 NMR study. RSC Advances 7(45), 28213–28223. https://doi.org/10.1039/C7RA03487C.
[6] Cedirian, S., Prudkin, L., Piraccini, B.M., Santamaria, J., Piquero-Casals, J., Saceda-Corralo, D., 2025. The exposome impact on hair health: etiology, pathogenesis and clinical features – Part I. Anais Brasileiros de Dermatologia 100(1), 131–140. https://doi.org/10.1016/j.abd.2024.07.003.
[7] Chatterley, A.S., Laity, P., Holland, C., Weidner, T., Woutersen, S., Giubertoni, G., 2022. Broadband Multidimensional Spectroscopy Identifies the Amide II Vibrations in Silkworm Films. Molecules 27(19), 6275. https://doi.org/10.3390/molecules27196275.
[8] Cruz, C.F., Costa, C., Gomes, A.C., Matamá, T., Cavaco-Paulo, A., 2016. Human Hair and the Impact of Cosmetic Procedures: A Review on Cleansing and Shape-Modulating Cosmetics. Cosmetics 3(3), 26. https://doi.org/10.3390/cosmetics3030026.
[9] Dragojlov, I., Aad, R., Ami, D., Mangiagalli, M., Natalello, A., Vesentini, S., 2025. Silk Sericin-Based Electrospun Nanofibers Forming Films for Cosmetic Applications: Preparation, Characterization, and Efficacy Evaluation. Molecules 30(3), 715. https://doi.org/10.3390/molecules30030715.
[10] Fernandes, C., Medronho, B., Alves, L., Rasteiro, M.G., 2023. On Hair Care Physicochemistry: From Structure and Degradation to Novel Biobased Conditioning Agents. Polymers 15(3), 608. https://doi.org/10.3390/polym15030608.
[11] Florou, V.A., Manaprasertsak, A., Slyusarenko, M., Amend, S.R., Kazi, J.U., Hammarlund, E.U., Pienta, K.J., 2025. Human hair as a diagnostic tool in medicine. Biochemistry and Biophysics Reports 43, 102129. https://doi.org/10.1016/j.bbrep.2025.102129.
[12] Grymowicz, M., Rudnicka, E., Podfigurna, A., Napierala, P., Smolarczyk, R., Smolarczyk, K., Meczekalski, B., 2020. Hormonal Effects on Hair Follicles. International Journal of Molecular Sciences 21(15), 5342. https://doi.org/10.3390/ijms21155342.
[13] Gvazava, N., Konings, S.C., Cepeda-Prado, E., Skoryk, V., Umeano, C.H., Dong, J., Silva, I.A.N., Ottosson, D.R., Leigh, N.D., Wagner, D.E., Klementieva, O., 2023. Label-Free High-Resolution Photothermal Optical Infrared Spectroscopy for Spatiotemporal Chemical Analysis in Fresh, Hydrated Living Tissues and Embryos. Journal of the American Chemical Society 145(45), 24796–24808. https://doi.org/10.1021/jacs.3c08854.
[14] Holman, A.P., Kurouski, D., 2023a. Role of Race/Ethnicity, Sex, and Age in Surface-Enhanced Raman Spectroscopy- and Infrared Spectroscopy-Based Analysis of Artificial Colorants on Hair. ACS Omega 8(23), 20675–20683. https://doi.org/10.1021/acsomega.3c01241.
[15] Holman, A.P., Kurouski, D., 2023b. Role of Race/Ethnicity, Sex, and Age in Surface-Enhanced Raman Spectroscopy- and Infrared Spectroscopy-Based Analysis of Artificial Colorants on Hair. ACS Omega 8(23), 20675–20683. https://doi.org/10.1021/acsomega.3c01241.
[16] Hu, H.M., Zhang, S.B., Lei, X.H., Deng, Z.L., Guo, W.X., Qiu, Z.F., Liu, S., Wang, X.Y., Zhang, H., Duan, E.K., 2012. Estrogen Leads to Reversible Hair Cycle Retardation through Inducing Premature Catagen and Maintaining Telogen. PLOS ONE 7(7), e40124. https://doi.org/10.1371/journal.pone.0040124.
[17] Hussein, R.S., Bin Dayel, S., Abahussein, O., El-Sherbiny, A.A., 2025. Influences on Skin and Intrinsic Aging: Biological, Environmental, and Therapeutic Insights. Journal of Cosmetic Dermatology 24(2), e16688. https://doi.org/10.1111/jocd.16688.
[18] Javarappa, K., Panchakshari, A., Renukaprasad, S., Pramod, M., 2026. Identification and Comparison of Functional Groups in Medicinal Plants using Attenuated Total Reflectance–Fourier Transform Infrared (ATR-FTIR) Spectroscopy. Journal of Asian Multicultural Research for Medical and Health Sciences Study. https://amrsjournals.com/jamrmhss/article/view/1095.

[19] Ji, Y., Yang, X., Ji, Z., Zhu, L., Ma, N., Chen, D., Jia, X., Tang, J., Cao, Y., 2020. DFT-Calculated IR Spectrum Amide I, II, and III Band Contributions of N-Methylacetamide Fine Components. ACS Omega 5(15), 8572–8578. https://doi.org/10.1021/acsomega.9b04421.

[20] Kaleta, M., Oklestkova, J., Novák, O., Strnad, M., 2021. Analytical Methods for the Determination of Neuroactive Steroids. Biomolecules 11(4), 553. https://doi.org/10.3390/biom11040553.Amet, E., Consectetur, F., 2022. Placeholder Text and Manuscript Formatting. Journal of Academic Templates 7(1), 1–15.

[21] Kalmodia, S., Parameswaran, S., Yang, W., Barrow, C.J., Krishnakumar, S., 2015. Attenuated Total Reflectance Fourier Transform Infrared Spectroscopy: An analytical technique to understand therapeutic responses at the molecular level. Scientific Reports 5(1), 16649. https://doi.org/10.1038/srep16649.

[22] Kathiresan, S., Meenakshisundaram, O., 2022. Effect of alkali treated and untreated cellulose fibers and human hair on FTIR and tensile properties for composite material applications. SN Applied Sciences 4(3), 74. https://doi.org/10.1007/s42452-022-04946-9.

[23] Li, C., Du, Y., Chen, H., Han, X., Wu, W., Kong, X., Zhang, C., Yuan, X., 2023. Transmission infrared micro-spectroscopic study of individual human hair. Journal of Biomedical Optics 28(11), 116501. https://doi.org/10.1117/1.JBO.28.11.116501.

[24] Madel, M.B., Niederstätter, H., Parson, W., 2016. TriXY—Homogeneous genetic sexing of highly degraded forensic samples including hair shafts. Forensic Science International: Genetics 25, 166–174. https://doi.org/10.1016/j.fsigen.2016.09.001.

[25] Malek, K., Wood, B.R., Bambery, K.R., 2014. FTIR imaging of tissues: Techniques and methods of analysis. Challenges and Advances in Computational Chemistry and Physics 14, 419–473. https://doi.org/10.1007/978-94-007-7832-0_15.

[26] Malinauskyte, E., Shrestha, R., Cornwell, P.A., Gourion-Arsiquaud, S., Hindley, M., 2021. Penetration of different molecular weight hydrolysed keratins into hair fibres and their effects on the physical properties of textured hair. International Journal of Cosmetic Science 43(1), 26–37. https://doi.org/10.1111/ics.12663.

[27] Mehra, S., Chadha, P., 2020. Alterations in structure of biomolecules using ATR-FTIR and histopathological variations in brain tissue of Channa punctatus exposed to 2-naphthalene sulfonate. Toxicology Research 9(4), 530–536. https://doi.org/10.1093/toxres/tfaa052.

[28] Mitu, B., Cerda, M., Hrib, R., Trojan, V., Halámková, L., 2023. Attenuated Total Reflection Fourier Transform Infrared Spectroscopy for Forensic Screening of Long-Term Alcohol Consumption from Human Nails. ACS Omega 8(24), 22203–22210. https://doi.org/10.1021/acsomega.3c02579.

[29] Mitu, B., Trojan, V., Halámková, L., 2023. Sex Determination of Human Nails Based on Attenuated Total Reflection Fourier Transform Infrared Spectroscopy in Forensic Context. Sensors 23(23), 9412. https://doi.org/10.3390/s23239412.

[30] Mujeeb, M., Zafar, M.K.M., 2017. FTIR spectroscopic analysis on human hair. International Journal of Innovative Research in Science, Engineering and Technology. Available at: https://manuu.edu.in/sites/default/files/Research-Publication/Translation/Khalid-Mubashir/FTIR-Spectroscopic-Analysis-on-Human-Hair.pdf.

[31] Philipsen, M.H., Haxen, E.R., Manaprasertsak, A., Malmberg, P., Hammarlund, E.U., 2021. Mapping the Chemistry of Hair Strands by Mass Spectrometry Imaging—A Review. Molecules 26(24), 7522. https://doi.org/10.3390/molecules26247522.

[32] Pienpinijtham, P., Thammacharoen, C., Naranitad, S., Ekgasit, S., 2018. Analysis of cosmetic residues on a single human hair by ATR FT-IR microspectroscopy. Spectrochimica Acta Part A: Molecular and Biomolecular Spectroscopy 197, 230–236. https://doi.org/10.1016/j.saa.2018.01.084.

[33] Portaccio, M., Faramarzi, B., Lepore, M., 2023. Probing Biochemical Differences in Lipid Components of Human Cells by Means of ATR-FTIR Spectroscopy. Biophysica 3(3), 524–538. https://doi.org/10.3390/biophysica3030035.

[34] Sharma, A., Verma, R., Kumar, R., Chauhan, R., Sharma, V., 2020. Chemometric analysis of ATR-FTIR spectra of fingernail clippings for classification and prediction of sex in forensic context. Microchemical Journal 159, 105504. https://doi.org/10.1016/j.microc.2020.105504.

[35] Swamy, P.M., Somashekar, P.H., Shivamurthy, S.A., Shadakshari, S., Puttaswamappa, M., Shanthappa, N.S., 2025. Design, synthesis, and in silico evaluation of 2-aminothiazole derivatives as potential mTOR and EGFR inhibitors. Discover Molecules 2(1), 31. https://doi.org/10.1007/s44345-025-00039-3.

[36] Szöllősi, A.G., Oláh, A., Bíró, T., Tóth, I., 2017. Recent advances in the endocrinology of the sebaceous gland. Dermato-Endocrinology 9(1). https://doi.org/10.1080/19381980.2017.1361576.

[37] Yang, F.C., Zhang, Y., Rheinstädter, M.C., 2014. The structure of people's hair. PeerJ 2014(1), e619. https://doi.org/10.7717/peerj.619.

[38] Zha, S., Wei, X., Fang, R., Wang, Q., Lin, H., Zhang, K., Zhang, H., Liu, R., Li, Z., Huang, P., Wang, Z., 2019. Estimation of the Age of Human Semen Stains by Attenuated Total Reflection Fourier Transform Infrared Spectroscopy: A Preliminary Study. Forensic Sciences Research 5(2), 119–125. https://doi.org/10.1080/20961790.2019.1642567.

[39] Zhao, T., Han, X., He, L., Jia, Y., Yu, R.C., 2023. Fourier Transform Infrared Spectrometry Detection of Phaeodactylum tricornutum Biomacromolecules in Response to Environmental Changes. ACS Omega 8(1), 702–708. https://doi.org/10.1021/acsomega.2c05933.

[40] Zhou, Y., Tao, L., Qiu, J., Xu, J., Yang, X., Zhang, Y., Tian, X., Guan, X., Cen, X., Zhao, Y., 2024. Tumor biomarkers for diagnosis, prognosis and targeted therapy. Signal Transduction and Targeted Therapy 9(1), 132. https://doi.org/10.1038/s41392-024-01823-2.